5th International Conference
on
Wind Turbine Noise
Denver 28-30 August 2013

Evaluation of Secondary Windshield Designs for Outdoor Measurement of Low Frequency Noise and Infrasound

Kristy Hansen, School of Mechanical Engineering, the University of Adelaide, North Tce., Adelaide, 5005, Australia,
kristy.hansen@adelaide.edu.au

Branko Zajamšek, School of Mechanical Engineering, the University of Adelaide, North Tce., Adelaide, 5005, Australia,
branko.zajamsek@adelaide.edu.au

Colin Hansen, School of Mechanical Engineering, the University of Adelaide, North Tce., Adelaide, 5005, Australia,
colin.hansen@adelaide.edu.au

Summary

In order to accurately characterise the noise measured in the vicinity of wind farms, it is necessary to ensure that outdoor microphones are adequately protected from the wind. A standard 90mm windshield is appropriate for measurements in light winds; however, as the wind speed increases, wind-induced pressure fluctuations erroneously contribute to the measured sound pressure level. Three alternative secondary windshields have been developed and tested in an outdoor environment and evaluated for their ability to allow low frequency noise and infrasound measurements to be obtained in the presence of wind. In addition, the effect of the microphone location with respect to the ground surface has been investigated for frequencies up to 1000 Hz. The measured sound pressure levels have been compared through analysis of high resolution frequency spectra and coherence for various wind conditions. Results show the presence of the wind turbine blade-pass frequency and its harmonics in the infrasonic range. In the low-frequency range, broadband peaks with superimposed secondary peaks spaced at the blade-pass frequency are evident. These spectral characteristics are further accentuated by stable atmospheric conditions. Results at low wind speed are also analysed to investigate the pressure doubling effect, in the context of low frequency noise, for all microphone mounting configurations. Comparison between the results using microphones with different secondary windshields mounted at ground level, at 1.5m and sub-surface in a box shows that there is no consistent difference between

measurements below 100Hz. This indicates that the 6dB correction may be relevant for any microphone location within a quarter of a wavelength from the ground.

1. Introduction

There are three main mechanisms responsible for the noise generated by modern wind turbines and the resulting sound spectra can be divided into overlapping frequency ranges (Vandenberg, 2011). Infrasound is produced when the airflow is slowed down by the presence of the wind turbine tower, rapidly changing the angle of attack of the air on the blade. It is characterised by tonal components at the blade-pass frequency and harmonics. Low frequency noise generation has been attributed to aerodynamic loading fluctuations which are caused by interaction between inflow turbulence and the rotating turbine blades (Hubbard & Shepherd, 1991). The level of inflow turbulence varies with atmospheric conditions and the noise source is broadband in nature with a maximum level at 10Hz. Higher frequency noise (500-1000Hz) is produced in response to rapid turbulent velocity fluctuations at the blade surface which cause sound generation at frequencies associated with these velocity fluctuations (Vandenberg, 2011).

At a typical residential location near a wind farm, the wind turbine noise spectrum is biased towards lower frequencies due to propagation effects (Leventhall, 2003). Attenuation of sound in air and attenuation due to reflection from a grass-covered ground both decrease with frequency and low frequencies are poorly absorbed by other obstacles as well. In addition, a house can behave as a low-pass filter, since the walls of a residence selectively block mid to high frequency noise. Hence, the determination of the levels of low frequency noise and infrasound at a residence is important when investigating the possible causes of annoyance.

It has been shown that the dominant source of pressure fluctuations for an outdoor microphone is the intrinsic turbulence in a flow rather than the fluctuating wake behind the windscreen (Morgan & Raspet, 1992). Since the wind velocity turbulence spectrum is heavily weighted to low frequencies, wind-induced noise is higher at low frequencies (Raspet *et al*., 2005). Consequently, it can be difficult to distinguish between wind turbine noise and wind-induced noise. This issue can be partially addressed by using a windshield, which reduces the atmospheric turbulence incident on the microphone. The effectiveness of the windshield can be further enhanced by using a secondary windshield which is separated from the primary windshield by a layer of air. The layer of air provides a region for viscous dissipation to reduce the turbulence generated behind the first windshield layer (Morgan & Raspet, 1991).

The international standard IEC 61-400 for wind turbine generator systems specifies use of a layered windshield design, where the secondary layer is hemispherical and the microphone is mounted to a circular board/plate. However, the layered windshield concept can also be incorporated into a spherical design. The advantage of spherically shaped windshields is that at low frequencies, the pressure fluctuations at the front and rear of the sphere are of opposite sign and thus cancellation occurs between these contributions, reducing the wind-induced noise at the centre of the sphere (Raspet *et al*., 2005). This cancellation would not occur for downward-travelling sound waves in a hemispherical windshield design and hence the sound field at the centre of the hemisphere would be different. The layered windshield design can also be achieved by using an underground box (Betke *et al*., 1996),

where the lid is replaced with a layer of acoustic foam, which is level with the ground to avoid the generation of turbulent eddies. This design minimises exposure to wind-induced noise and eliminates wake-induced turbulence.

The three layered-windshield designs discussed above were compared by analysing coherence between microphone measurements using the hemispherical and box windshields, hemispherical and spherical windshields and the box and spherical windshields for various wind conditions. It is reasonable to assume that the wind-induced noise at each microphone would be uncorrelated with that at the other microphones for each microphone due to differences in the secondary windshield geometry and differences in location, which would alter the turbulent interaction. Hence, it was deduced that a high coherence could indicate that the noise was associated with the operation of the wind farm. The coherence analysis was used to complement a high resolution narrowband analysis to identify potentially audible low-frequency noise not induced by the wind. A comparison between noise spectra from the different microphones was made to determine if the 6dB correction specified in the IEC 61-400 standard could be applicable to the other windshield configurations at low frequencies.

2. Methodology

2.1 Field measurements. Outdoor measurements were carried out for 6 days at a residence located approximately 1km north of the nearest turbine of a South Australian wind farm, which is made up of 37 operational turbines. The microphones were located approximately 5m from the residence and as far as possible (~10m) from the nearest trees, which were around 5m in height. Some small bushes and shrubs were located within a few metres of the microphones. Time series data were acquired using a National Instruments data acquisition device at a sampling rate of 10,200Hz for a continuous sequence of 10-minute samples. All microphones attached to this device were G.R.A.S type 40AZ with 26CG preamplifiers with a noise floor of 16dB(A) and a low frequency limit of 0.5Hz. The local wind speed and direction were measured concurrently at 1.5m and 10m using a Davis Vantage Vue and a Davis Vantage Pro weather station, respectively, capable of measuring to an accuracy of 0.4m/s. The weather stations were located around 20m from the residence in an open field and are pictured in Figure 1a. The wind data were averaged over 10-minute sample periods.

All three outdoor microphones were equipped with 90mm-diameter windshields as well as secondary windshields of various configurations. One microphone was positioned at ground level, another was mounted at a height of 1.5m, and the third was located underground inside a small plywood box.

The microphone at ground level pictured in Figure 1b was taped horizontally at the centre of a 1m diameter aluminium plate of 3mm thickness and covered by both a primary and secondary windshield as specified in the IEC 61400-11 standard. The secondary windshield consisted of a 16mm layer of acoustic foam, covered by a layer of SoundMaster acoustic fur. The windshield was riveted to the aluminium plate and secured with a pin.

The microphone pictured in Figure 1d was mounted at a height of 1.5m using a star-dropper to minimise wind noise interference associated with the more conventional method of tripod mounting. This microphone was fitted with a secondary spherical

windshield which was attached to a steel frame of diameter 450mm as shown in Figure 1d. The windshield materials were identical to those used for the hemispherical secondary windshield described above.

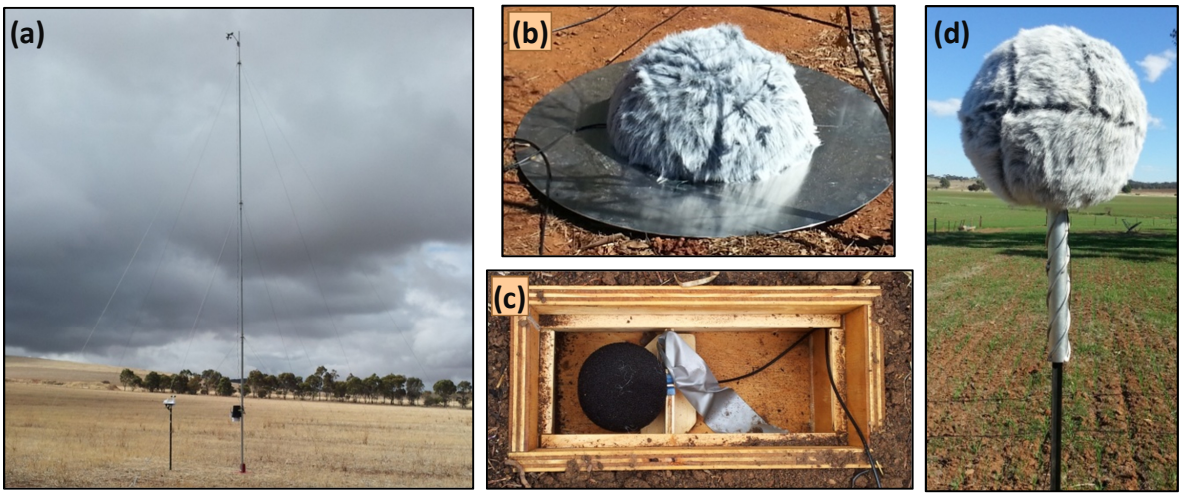

Figure 1 – (a) Davis weather stations at 1.5m and 10m, (b) Hemispherical windshield, (c) box windshield and (d) spherical windshield

The underground microphone pictured in Figure 1c was located in a 120mm x 120mm x 280mm plywood box with an acoustic foam lid, 50mm thick. The acoustic foam had a pore size of 20ppi. The top of the lid was flush with the surrounding ground to minimise the formation of eddies that would generate extraneous noise. The microphone was mounted horizontally on a custom-made shelf, which incorporated a hemispherical groove covered with a 3mm layer of rubber. This method of locating a microphone in an underground box to minimise wind noise was conceived by Betke (1996).

2.2 Wind shield Insertion losses. The anechoic chamber at the University of Adelaide, which has dimensions 4.79m x 3.90m x 3.94m, was used to measure the insertion loss of various microphone windshield configurations. A loudspeaker was located in one corner of the anechoic chamber and a microphone was located in the opposite corner. The loudspeaker generated pure tones at the third octave band centre frequencies, where the sound pressure level exceeded the background noise in the anechoic chamber by at least 15dB for all frequencies greater than 30Hz. The microphone position was kept constant to within ±50mm for measurements with the hemispherical windshield and box. In the case of the spherical windshield, the vertical position was shifted by 700mm due to the design of the mount but the horizontal distance from the speaker was not varied. The configurations tested are shown in Table 1 and the results are plotted in Figure 2.

Table 1 – Windshield configurations used in insertion loss experiments

	Test 1	Test 2	Reference test (ref)
Hemispherical windshield	Field configuration	No windshield, on aluminium plate	No windshield, on floor of anechoic chamber
Spherical windshield	Field configuration (without-star dropper)	-	No windshield, mounted 700mm from ground
Box with acoustic foam lid	Field configuration (above ground)	No windshield, in box	No windshield, on floor of anechoic chamber

The windshield with the most negligible insertion loss over the frequency range from 30Hz to 1000Hz is the spherical windshield. The hemispherical windshield has negligible insertion loss below 80Hz. From this frequency onwards, the negative insertion loss is associated with the presence of the plate. However, it should be noted that the value of the insertion loss is not 6dB since the wavelength of sound at low frequencies is much larger than the 1m diameter aluminium plate. The pressure doubling effect would be expected if the plate was placed on hard ground with a large enough surface area. The box shows negligible insertion loss below 160Hz. At higher frequencies, the negative insertion loss for the box seems to indicate the presence of standing waves. However, this is difficult to justify, as the first resonance frequency of the box is about 600 Hz.

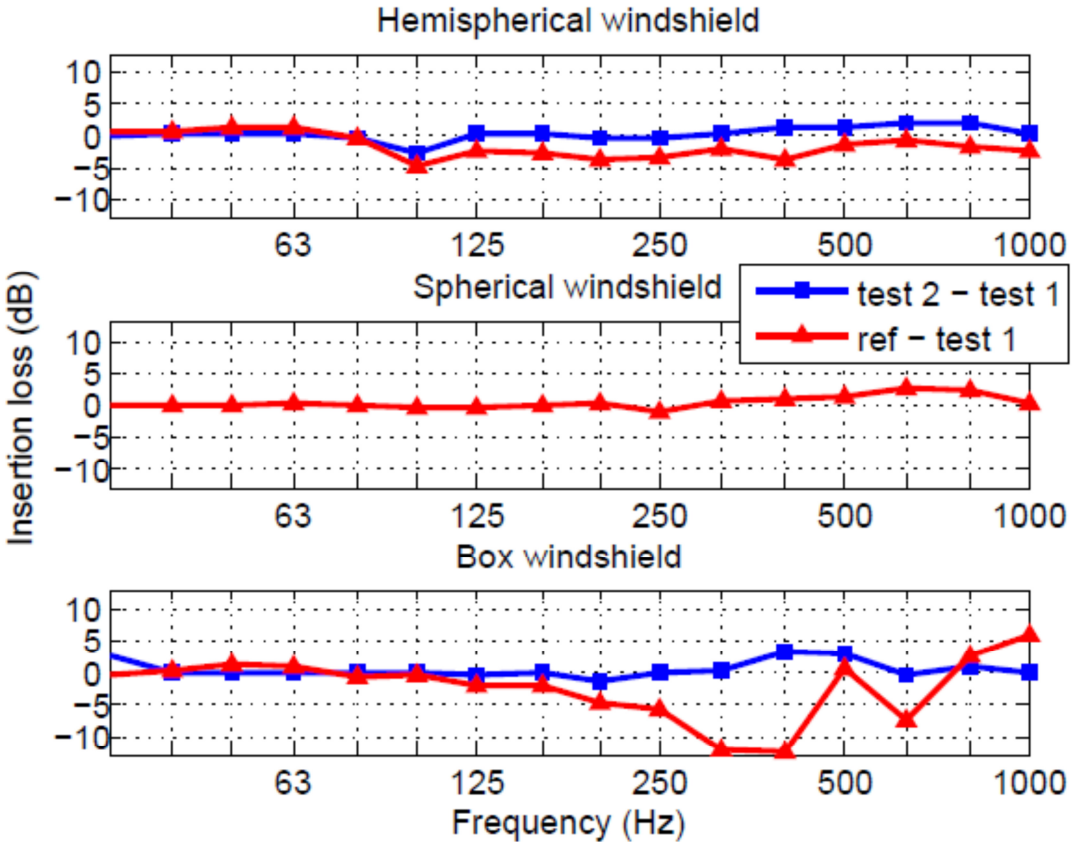

Figure 2 – Insertion loss for hemispherical, spherical and box windshields. The legend refers to all subplots using the test specifications outlined in Table 1.

3. Results

The data collected at night time are the main focus of this paper as there was some noise from farming machinery during the day. Nevertheless, daytime data are plotted for comparative purposes. The overall unweighted noise levels over the frequency range of 0-200Hz are plotted in Figure 3 as a function of time for the 6-day analysis period. These results were calculated by applying a 6th order low-pass Butterworth filter (with a cut off frequency of 200Hz) to the raw time data and then finding the root mean squared sum for each 10 minute measurement. There was negligible difference between the results for this low frequency range and results calculated over the frequency range of 0-1000Hz, indicating that the measured linear spectra are dominated by low frequency noise. The wind speed and direction at 1.5m and 10m are included in the figure to show how these variables affect the overall noise levels. It can be seen that the overall unweighted noise level increased with increased wind speed but that the wind direction did not significantly affect the results. It should be noted, however, that downwind conditions only occurred during the daytime and that these daytime results should be viewed with caution due to the farming machinery noise.

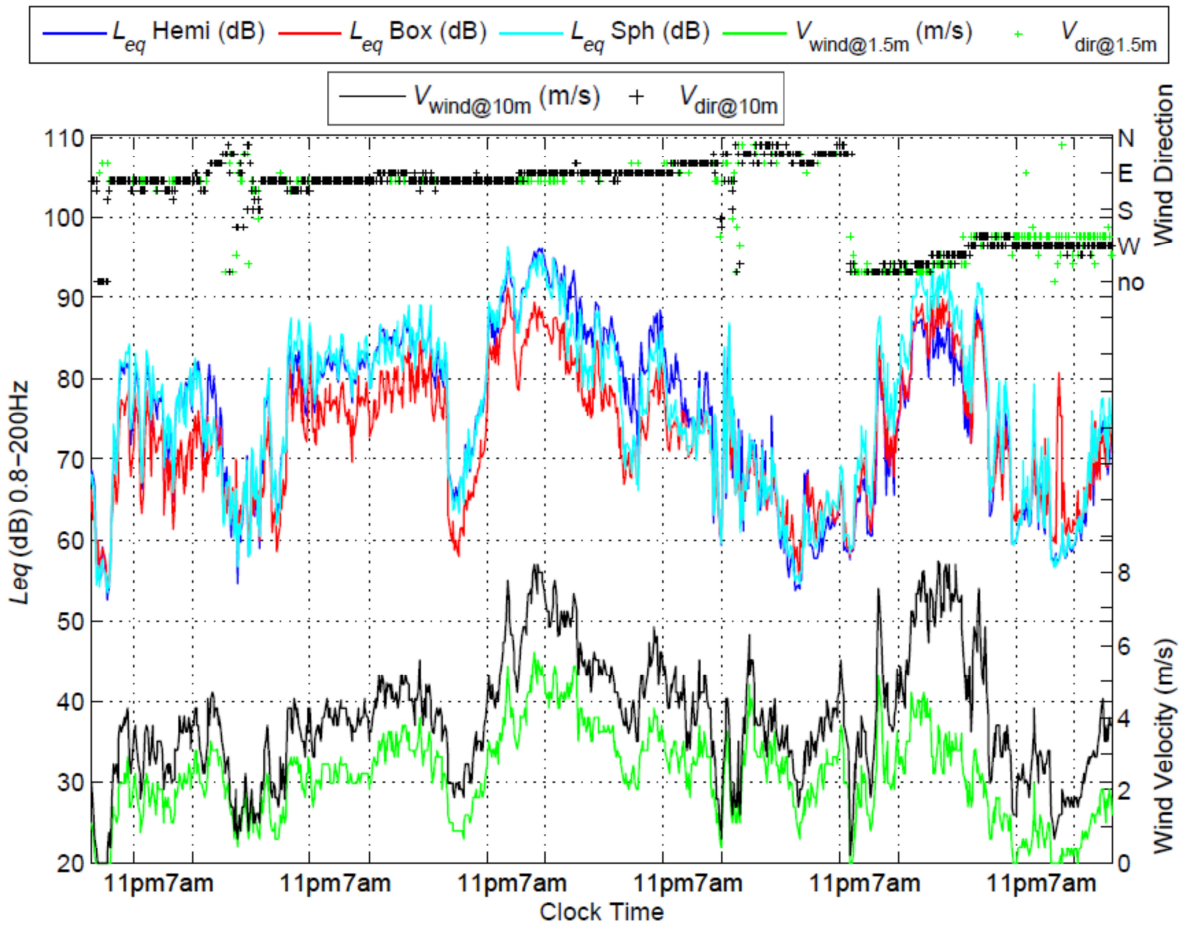

Figure 3 – Unweighted equivalent sound pressure level (L_{eq}) up to 200Hz for three microphones with a hemispherical, box and spherical windshield, respectively. The wind speed and direction at 1.5m and 10m is also shown in green and black, respectively.

Comparisons between the overall unweighted sound pressure level measured using different windshields reveals that the general trends are the same. However, the box windshield microphone consistently measured a lower sound pressure level and the hemispherical and spherical windshield microphones gave the most similar results. Differences between the results are attributed to interaction between atmospheric turbulence and the windshields which is influenced by windshield geometry and mounting location. Further insight can be gained by plotting the frequency spectrum results, as discussed later in this section.

To predict when wind turbine noise may have been most noticeable, an atmospheric stability plot was constructed. The value of m is determined from Equation 1, which was proposed by Kühner (1998) and used in the German Air Quality Guideline "TA-Luft" (1986).

$$m = \frac{log(v_h/v_{ref})}{log(h/h_{ref})} \quad (1)$$

This equation shows a relationship between the wind speed v_h at height h and the reference wind speed v_{ref} at a reference height h_{ref} which is governed by the atmospheric stability. Stability classes are outlined in detail in van den Berg (2004) where it was also shown that the contrast between ambient noise and wind turbine noise was greatest under stable conditions. Figure 4 shows the variation of stability with time over the 6-day measurement period. As hub-height wind speed data were unavailable, the m factor was calculated using the weather station data from 1.5m and 10m close to the microphone locations. It can be seen that conditions were the most stable on the sixth night and hence, this was selected as a time period for more detailed analysis. For comparison, the third night was chosen, as the conditions were least stable on this night.

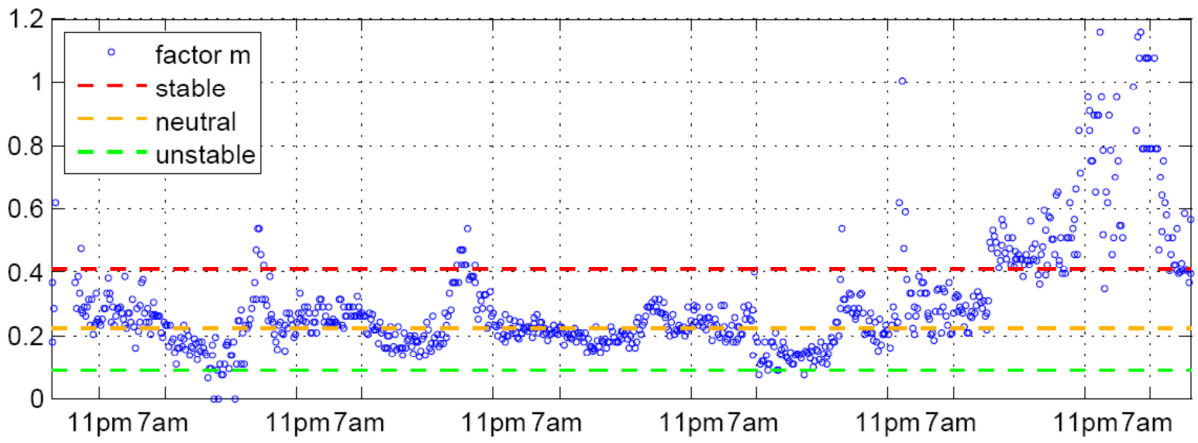

Figure 4 – Factor m plotted over the measurement period where stability classes are indicated with dashed lines.

A comparison between the overall unweighted, A-weighted and G-weighted sound pressure levels is shown in Figure 5 for the microphone in the hemispherical windshield. The overall unweighted level was calculated up to 200Hz since there was negligible increase when the frequency range was increased. The overall G-weighted level was determined up to the maximum frequency for which it is specified of 315Hz. The overall A-weighted level was calculated up to the maximum allowable

frequency for the sampling rate of 8192Hz (f_{max} = 4096Hz). The A-weighting is outlined in many regulations and standards for specifying allowable levels produced by wind farms (see for example the South Australian EPA document (EPA, 2009). The G-weighting is intended to reflect human perception of infrasonic noise (ISO-7196). Note that the measurement location was 1km from the nearest turbine in a direction ranging from N to NNW from the wind farm.

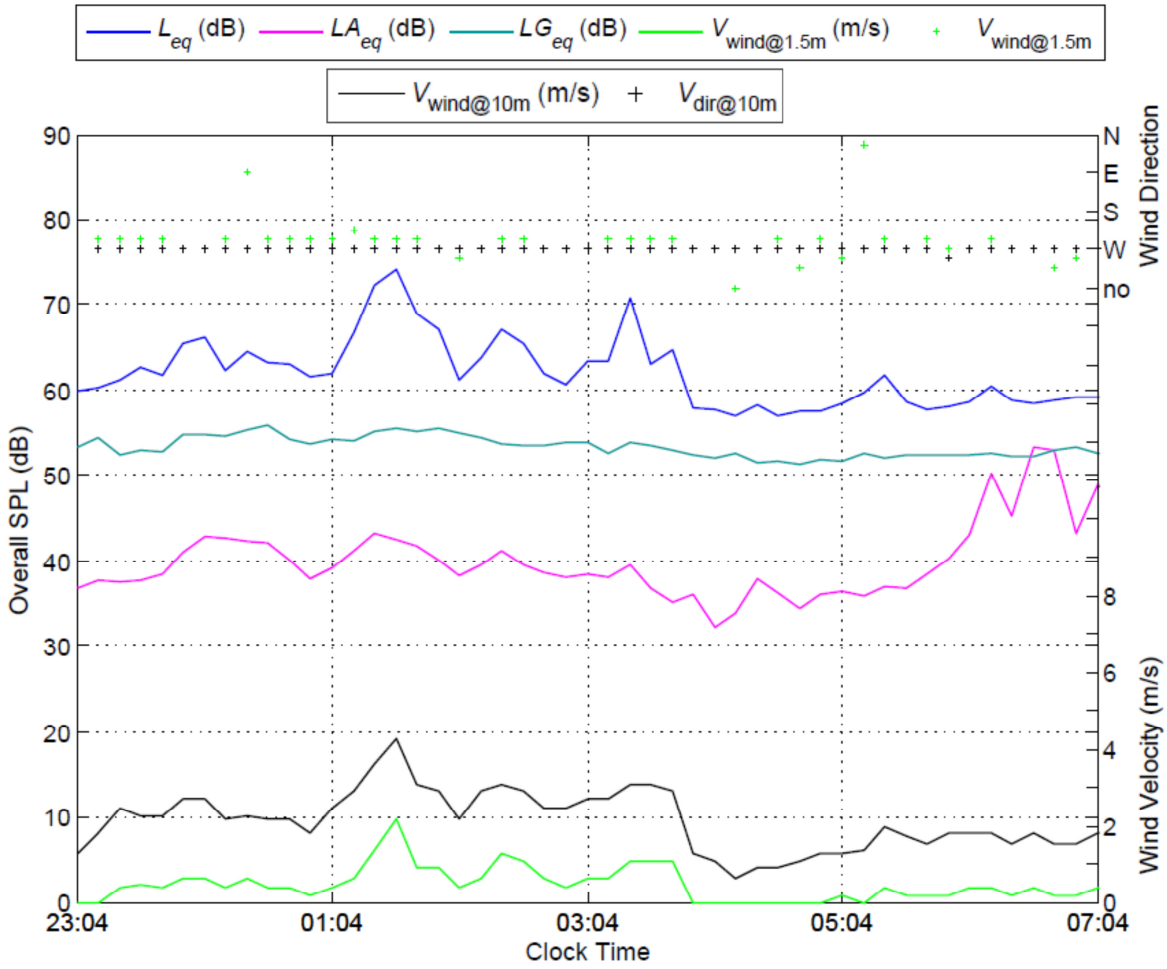

Figure 5 – Comparison between the overall unweighted, A-weighted and G-weighted sound pressure levels on the sixth night of measurement. The wind speed and direction at 1.5m and 10m is also shown in green and black, respectively.

There is a strong relationship between wind speed variations and fluctuations in the unweighted noise level, which is less significant for the A-weighted levels and negligible for the G-weighted levels. However, while it appears that applying a weighting function reduces the contribution of wind noise to the measurement, it should also be noted that power output from the wind farm was at a maximum at 1:24am, exactly when the unweighted noise level was highest as shown in Figure 6.

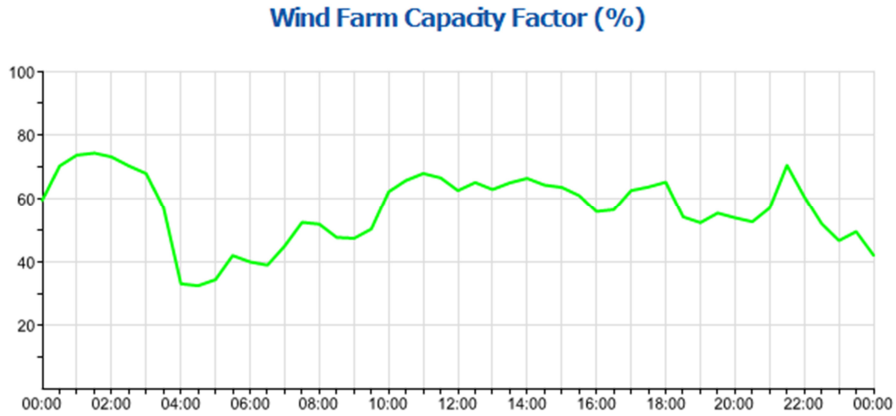

Figure 6 – Wind farm capacity factor for a South Australian wind farm on 22nd May 2013. Maximum capacity is 129MW (http://windfarmperformance.info/).

In order to establish the contribution of various frequencies to the overall unweighted noise level, third-octave spectra were plotted for the three microphones as shown in Figure 7. Two times were selected for the least stable night (Figure 7a, b) and the most stable night (Figure 7c, d), respectively. In the former case, the times were selected randomly and in the latter case, they were chosen to show when the measurements appeared to be most affected by the wind farm noise. The reference threshold of human hearing according to ISO 389-7 (2005) is also shown on the figures.

It can be seen in Figure 7b that the sound pressure level (SPL) of infrasound is relatively high, especially below 10Hz. There are some minor peaks around 31.5Hz and 50Hz but these are less than 3dB above the levels for the adjacent third-octave bands. In Figure 7c, the level of infrasound is much lower and the peaks at 31.5Hz and 50Hz are more evident. The results for the various windshield configurations show that there is better agreement between the three microphones in Figure 7a than in Figure 7b, which indicates that the microphones are measuring less wind-induced noise at this time. This is consistent with the fact that the wind speed on 19th April at 0:14 is approximately half of the value measured at 6:34. The box windshield configuration shows the lowest infrasonic levels in Figure 7a and Figure 7b, which implies that this windshield performs best in windy conditions. This is consistent with the fact that the wind-induced turbulence is expected to be lower sub-surface. The spherical windshield measures the lowest infrasound on the windiest night, according to Figure 7b. According to these results and the results shown in Figure 3, it can be seen that this windshield is at least as effective as the hemispherical design. A larger data set would need to be analysed to determine if the spherical windshield consistently measured lower levels of infrasound in windy conditions.

On the night of the 21st April, the wind speed was much lower at 1.5m and third-octave spectra plots depicted in Figure 7c and d show lower levels of infrasound. On the other hand, the peak levels are up to 10dB above the levels for adjacent frequency bins. The infrasonic peak frequencies are in the range of the blade-pass frequency which is typically 0.5-1.5Hz for modern wind turbines. The peak levels at 25Hz and 50Hz are much more significant in Figure 7c and d and are as high as 20dB above the adjacent frequency bin levels. It is also evident that the unweighted levels measured using different windshield configurations are in excellent agreement, which is expected for light-wind conditions.

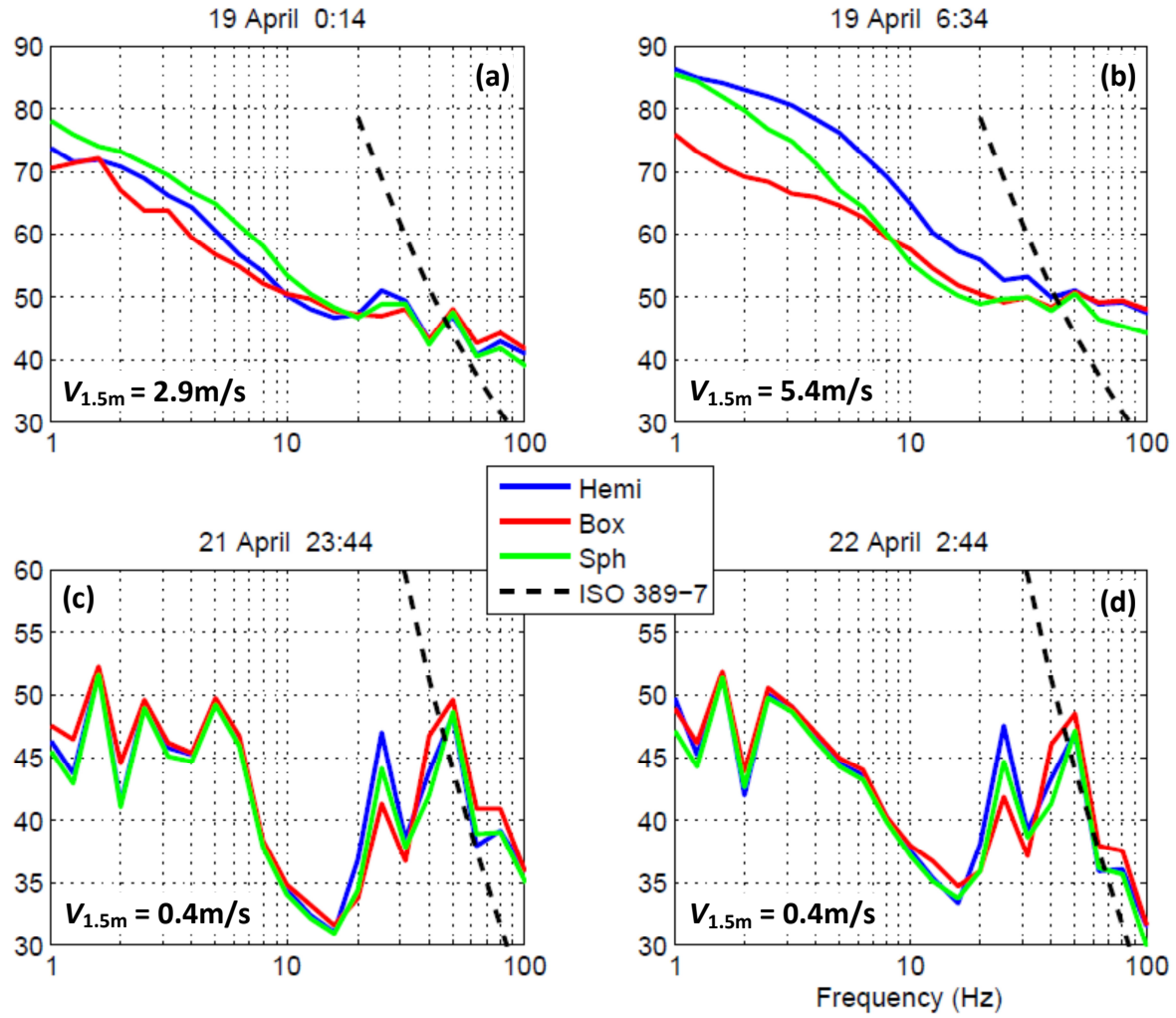

Figure 7 – Spectrum plots showing significant variations between measurements with identical field set-up on different nights. Results are presented for microphones with a hemispherical, box and spherical windshield and the ISO 389-7 curve is shown for comparison.

Although analysis of the third-octave levels provides a good overview of the variation in sound pressure level with frequency, more detailed information is lost. Hence, a narrowband analysis was carried out with a frequency resolution of 0.1Hz. The results are plotted in Figure 8 and Figure 9 for the worst case and reference case, respectively. The figures are separated into the infrasound region in (a) and the low-frequency region in (b).

In Figure 8a, the harmonics of the blade-pass frequency of 0.8Hz are clearly reflected in the spectral plot up to around 9.6Hz. On the other hand, the blade-pass frequency itself is indistinguishable. The narrowband analysis reveals a significant amount of information in Figure 8b that was not visible on the third-octave plot. The spectral peaks that were identified in the third-octave plots are rather visible as a broadband hump. Also, secondary peaks that have a spacing corresponding to the blade-pass frequency are evident throughout the spectrum, especially on the broadband humps. According to international standard ISO 389-7 (2005), which specifies the threshold of hearing for free-field tonal noise, the peaks near 43Hz,

50Hz, 68Hz and 74Hz would be just perceptible, but the peak at 23.5 Hz should not be audible to a person with normal hearing.

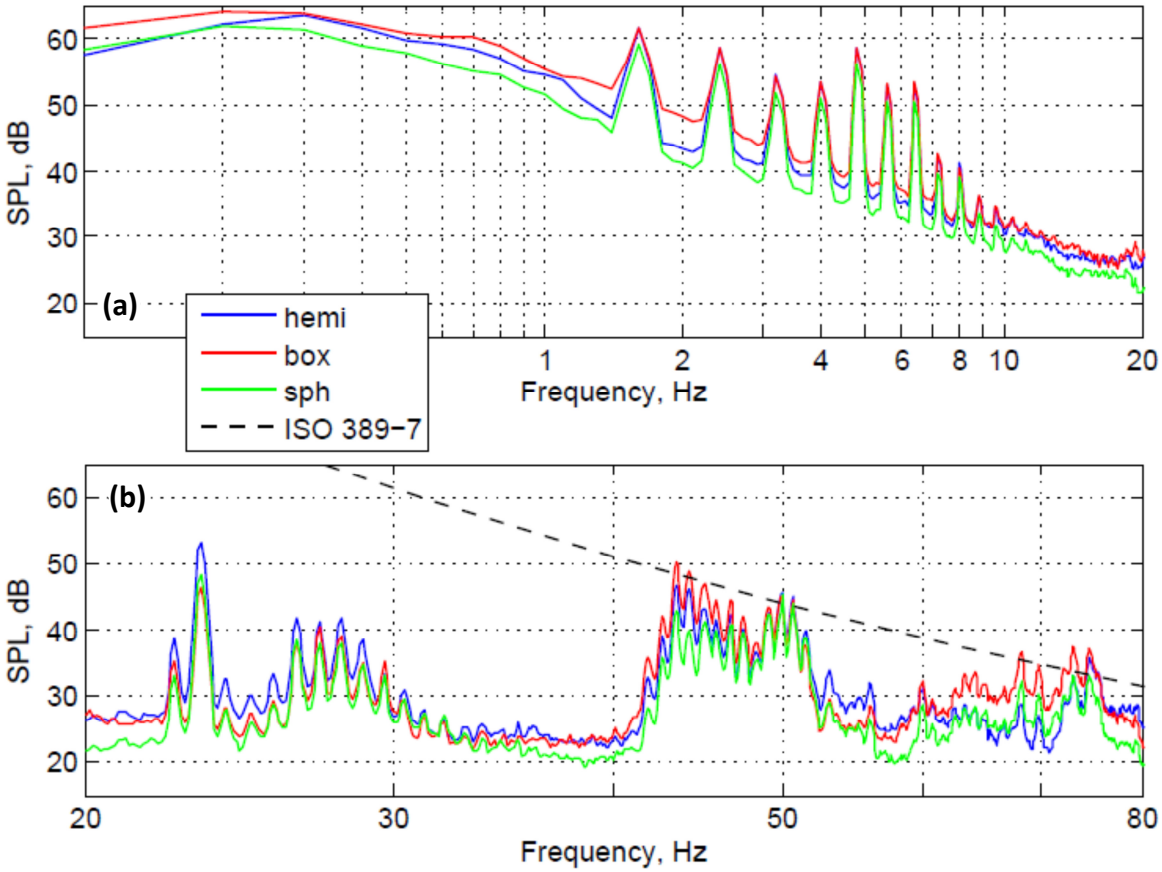

Figure 8 – Narrowband spectra with frequency resolution of 0.1Hz for 21st April at 23:44. Results are presented for microphones with a hemispherical, box and spherical windshield and the ISO 389-7 curve is shown for comparison.

Comparison between the results for the different windshield configurations in Figure 8 indicates that there are slight variations in the peak sound pressure level but the position of the peaks with respect to frequency is consistent. In this case, the level of infrasound measured by the box windshield microphone is slightly higher than for the other windshield configurations. This indicates that the box windshield is only advantageous in windy conditions. It is also evident that the sound pressure level measured with the hemispherical windshield is not consistently 6dB higher than the other measurements. Hence, it is probable that positive reinforcement between the incident and reflected waves at low frequencies occurs not only at the ground, but also at a height of 1.5m. In this case the pressure-doubling and hence 6dB correction would be relevant for both microphone receivers.

Figure 9 is a plot of the sound pressure level against frequency for the reference case microphone measurements with the hemispherical, box and spherical windshield configurations. Peaks at the blade-pass frequency are still present in Figure 9a but are much smaller relative to adjacent levels. This is attributed to increased levels of infrasound associated with the higher wind speed. The reason that the peaks are visible at higher levels than those in Figure 8a is that the wind farm was producing more power at this time. The nature and position of the peaks

with respect to frequency is similar in Figure 8b and Figure 9b. However, the superposition of the blade-pass frequency is less evident. Nevertheless, the peak around 75Hz, which is at a similar level to the same peak in Figure 8b, could be audible to people with normal hearing according to ISO 389-7 (2005).

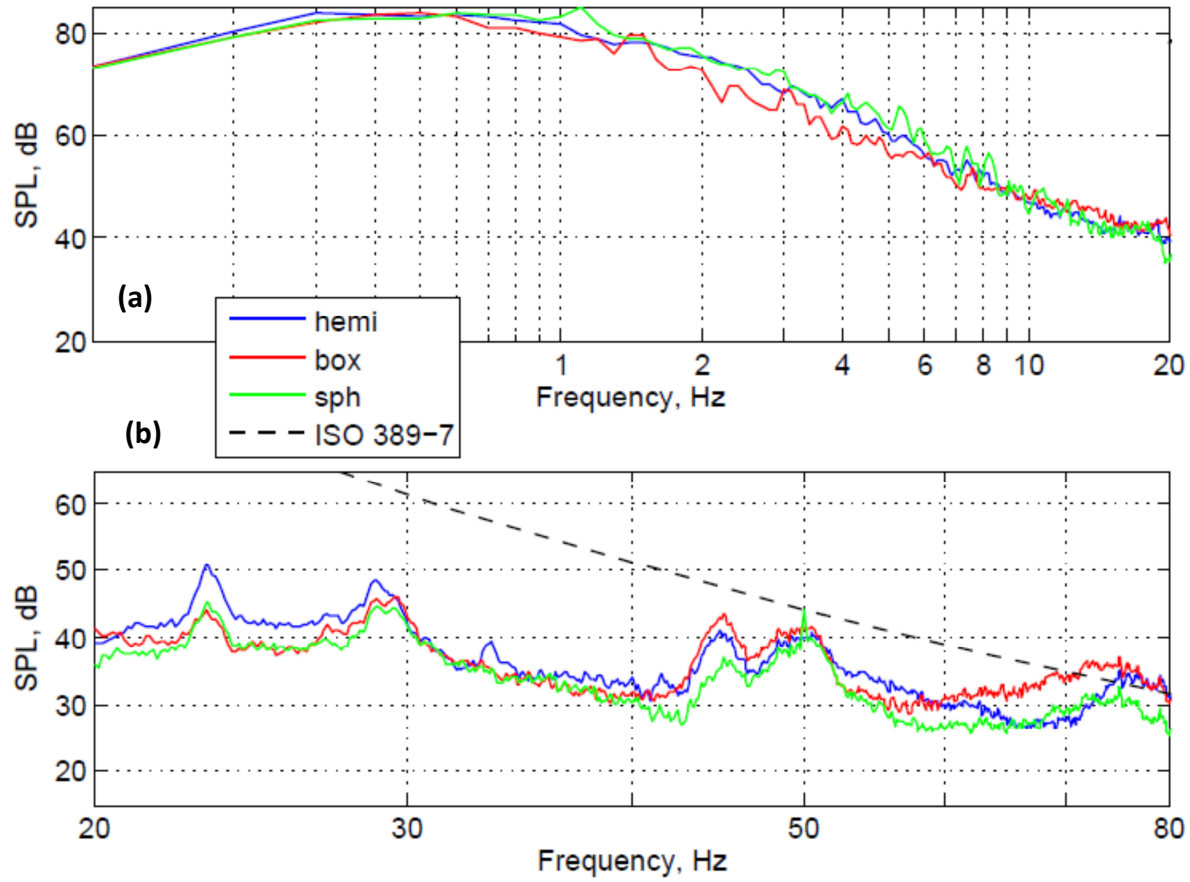

Figure 9 – Narrowband spectra with frequency resolution of 0.1Hz for 19th April at 0:14. Results are presented for microphones with a hemispherical, box and spherical windshield and the ISO 389-7 curve is shown for comparison.

The coherence is used to determine the existence or otherwise of a relationship between data sets for the different windshield configurations. To improve the accuracy of the coherence method a 6th order Butterworth low-pass filter (with a cut off frequency of 100Hz) was used to maximise the signal-to-noise ratio. Coherence plots with a frequency resolution of 0.1 Hz are shown in Figure 10 and Figure 11 for the infrasonic and low-frequency ranges. These figures show the coherence between microphone measurements using the hemispherical and box windshields, hemispherical and spherical windshields and the box and spherical windshields. In Figure 10, coherence is high for the harmonics of the blade-pass frequency as well as for the peaks around 23Hz, 27Hz, 45Hz and 73Hz and the adjacent secondary peaks spaced at the blade-pass frequency of 0.8Hz.

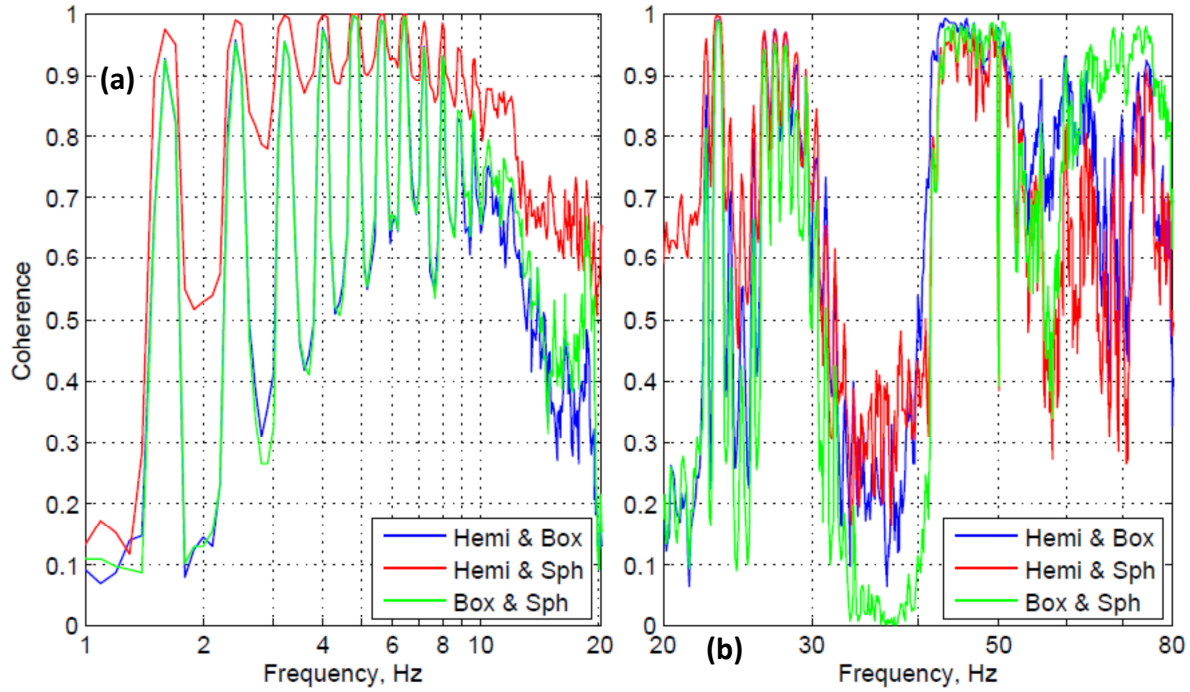

Figure 10 – Coherence between microphone measurements using the hemispherical, box and spherical windshields on 20th April at 23:44. The frequency resolution was 0.1Hz.

In general, the signals are less coherent for the data shown in Figure 11, especially in the infrasonic range. This indicates that wind-induced noise dominates the signal at these frequencies, and increased sound level at the blade-pass frequency cannot be distinguished. The signals tend to be coherent at the centre frequency of the broadband peaks but then drop rapidly due to reduced influence of the blade-pass frequency on the signals.

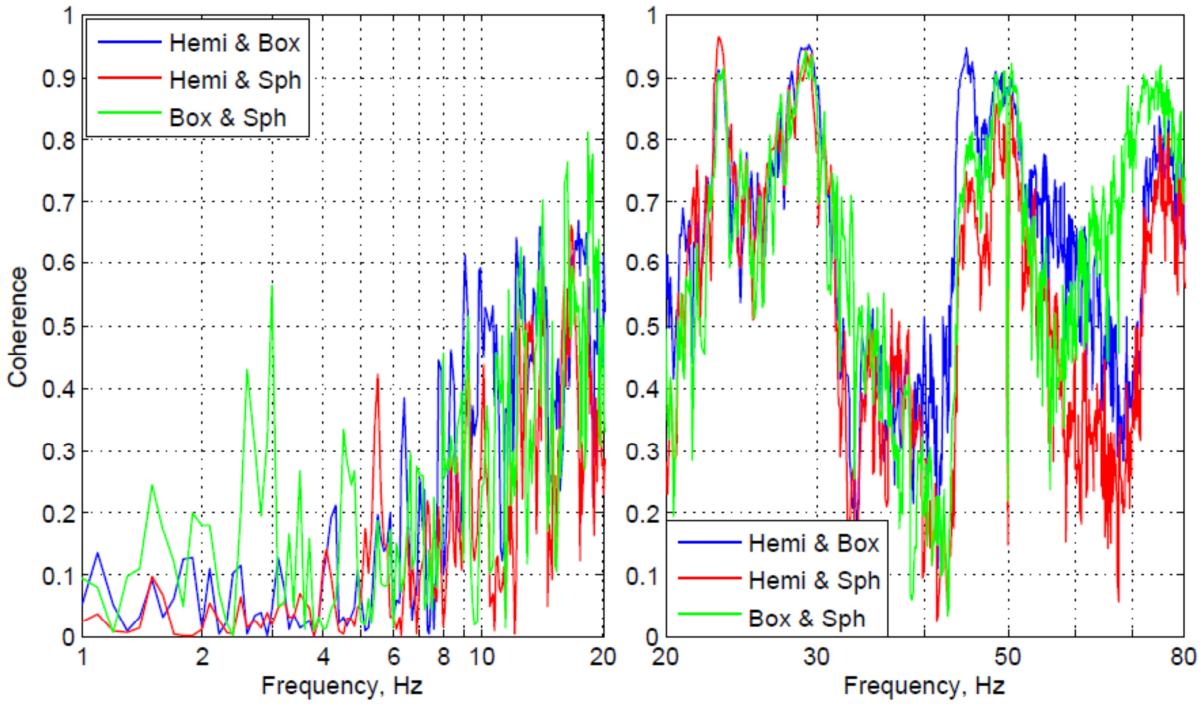

Figure 11 – Coherence between microphone measurements using the hemispherical, box and spherical windshields on 19th April at 0:14. The frequency resolution was 0.1Hz.

3. Conclusions

For the different windshield configurations investigated in this study, there is good agreement between measurements at low frequencies, particularly for stable atmospheric conditions. Under these conditions, at a distance of 1 km in a downwind direction of north from the nearest turbine in the wind farm, the harmonics of the blade-pass frequency are clearly visible in the infrasonic spectral plots. In the low-frequency range, broadband peaks are present for the majority of the measurement period. However, under stable conditions, these broadband peaks are superimposed with secondary peaks spaced at the blade-pass frequency, which increases the noise level at these frequencies. The resultant noise is at a level that can be perceived by humans, according to ISO 389-7 (2005).

Investigation into the influence of microphone mounting configuration on the results shows that below 100Hz, there are no consistent differences in the spectral results. Hence, it is deduced that at low frequencies, pressure doubling could occur both at the ground and at 1.5m, due to the large wavelengths involved. For windy conditions, the box windshield configuration appears to be least affected by wind-induced noise.

References

Betke K, Schults von Glahn, M and Goos, O (1996) Measurement of infrasound emitted by wind turbines (in German) Proceedings of DEWEK, 207–210.

H.H. Hubbard HH and K.P. Shepherd KP (1991) Aeroacoustics of Large Wind Turbines Journal of Acoustical Society of America 89(6), 2495-2508.

International Organization for Standardization, ISO 7196 (1995) Acoustics – Frequency-weighting characteristic for infrasound measurements ISO, Geneva.

International Organization for Standardization, ISO 389-7 (2005) Reference threshold of hearing under free-field and diffuse-field listening conditions ISO, Geneva.

Kühner, D (1998) Excess attenuation due to meteorological influences and ground impedance Acustica—Acta Acustica 84, 870–883.

Leventhall, G (2003) A review of published research on low frequency noise and its effects Defra Publications, London.

Morgan, S and Raspet, R (1991) Investigation of the mechanisms of low-frequency wind noise generation outdoors Journal of Acoustical Society of America 92(20), 1180-1183.

Raspet, R, Webster, J and Dillon, K (2005) Framework for wind noise studies Journal of Acoustical Society of America 119(2), 834-843.

TA-Luft, Erste Allgemeine Verwaltungsvorschrift zum Bundes-Immissionsschutzgesetz – Technische Anleitung zur Reinhaltung der Luft (First general directive to the federal immission protection act—Technical guideline for clean air), 1986 (in German).

van den Berg, GP (2004) Effects of wind profile at night on wind turbine sound Journal of Sound and Vibration 277, 955-970.

van den Berg, GP (2011) The beat is getting stronger Noise Notes 4(4), 15-40.